

1 **Identification of a novel antimicrobial peptide from the sea star *Patiria pectinifera***

2 Chan-Hee Kim^{a,1}, Hye-Jin Go^{a,1}, Hye Young Oh^a, Ji Been Park^a, Tae Kwan Lee^a, Jung-Kil Seo^b,
3 Maurice R. Elphick^c, and Nam Gyu Park^{a,*}

4 ^aDepartment of Biotechnology, College of Fisheries Sciences, Pukyong National University, Busan
5 48513, Korea

6 ^bDepartment of Food Science and Biotechnology, Kunsan National University, Kunsan 54150, Korea

7 ^cSchool of Biological and Chemical Sciences, Queen Mary University of London, London, E1 4NS UK

8

9

10 *Correspondence to: N. G. Park, Department of Biotechnology, College of Fisheries Sciences,
11 Pukyong National University, 45 Youngso-ro, Nam-gu, Busan, 48513, Korea; Tel.: +82-51-629-
12 5867; Fax: +82-51-629-5863; *E-mail*: ngpark@pknu.ac.kr (N.G. Park)

13

14

15

16 **Running title: *PpCrAMP*: a novel sea star cysteine-rich antimicrobial peptide**

17

18

19

20 Footnotes: ¹These authors contributed equally to this work.

21

22

23

24 Abbreviations: AMPs, antimicrobial peptides; MALDI-TOF MS, matrix assisted laser
25 desorption/ionization time-of-flight mass spectrometry; DTT, 1,4-dithiothreitol; TSB, tryptic soy
26 broth; CFU, colony forming unit; RACE, rapid amplification of cDNA ends; *PpCrAMP*, *Patiria*
27 *pectinifera* cysteine-rich antimicrobial peptide; TFA, trifluoroacetic acid; RP, reversed-phase; RT-
28 qPCR, real-time quantitative polymerase chain reaction.

29 **Abstract**

30 Antimicrobial peptides (AMPs) are components of innate immunity found in many forms of life.
31 However, there have been no reports of AMPs in sea star (Phylum Echinodermata). Here we report
32 the isolation and characterization of a novel antimicrobial peptide from the coelomic epithelium
33 extract of the sea star *Patiria pectinifera*. The isolated peptide comprises 38 amino acid residues, is
34 cationic (pI 9.2), has four cysteine residues that form two disulfide bonds (C1-C3 and C2-C4), is
35 amidated at the C-terminus, and is designated *P. pectinifera* cysteine-rich antimicrobial peptide
36 (*PpCrAMP*). Synthetic *PpCrAMP* identical to the native peptide exhibited the most potent
37 antimicrobial activity compared to analogs with different disulfide bond configurations. Expression
38 analysis of *PpCrAMP* precursor transcripts revealed constitutive expression in the coelomic
39 epithelium and tube feet of *P. pectinifera*. Analysis of genomic DNA and cDNA encoding the
40 *PpCrAMP* precursor protein revealed that an intron splits the coding region of the mature peptide into
41 a positively charged N-terminal domain and a C-terminal domain harboring four cysteine residues and
42 a glycine for C-terminal amidation. No significant homology with other known AMPs was observed,
43 while orthologs of *PpCrAMP* were found in other echinoderm species. These findings indicate that
44 *PpCrAMP* is the prototype of a family a novel cysteine-rich AMPs that participate in mechanisms of
45 innate immunity in echinoderms. Furthermore, the discovery of *PpCrAMP* may lead to the
46 identification of related AMPs in vertebrates and protostome invertebrates.

47

48 **Keywords:** sea star, *Patiria pectinifera*, cysteine-rich antimicrobial peptide, innate immunity,
49 echinoderm

50 **1. Introduction**

51 Antimicrobial peptides (AMPs) are evolutionarily ancient molecules produced by a wide variety
52 of organisms (Ganz, 2003; Zasloff, 2002). AMPs are a major component of the immune defense
53 system in invertebrates, which lack a vertebrate-type adaptive immune system (Bulet et al., 2004;
54 Sperstad et al., 2011). Although AMPs exhibit structural diversity, they are commonly defined as
55 being short (10-50 amino acids, AAs) with a net positive charge (+2 to +9) and have been classified
56 into three major groups: (i) linear peptides that form amphipathic α -helices, (ii) cysteine-rich peptides
57 containing one or more disulfide bonds and (iii) peptides with an overrepresentation of one or two
58 AAs (Bulet et al., 2004; Hancock and Lehrer, 1998; Wang et al., 2016; Zasloff, 2002). The peptides
59 are derived from larger precursor proteins (prepropeptides) that consist of a signal peptide, a
60 prosequence, and a mature peptide (Bulet et al., 2004; Liu and Ganz, 1995; Valore and Ganz, 1992).
61 AMPs are not only characterized by direct antibiotic, antifungal, and antiviral activity against a
62 variety of microorganisms but are also involved indirectly in modulation of the innate immunity,
63 including induction of chemokine production and regulation of apoptosis, angiogenesis, and wound
64 healing (Bowdish et al., 2005; Ganz, 2003; Guilhelmelli et al., 2013; Hancock and Sahl, 2006;
65 Oppenheim and Yang, 2005). Because of the development of antibiotic resistance by microorganisms,
66 AMPs have attracted considerable attention in recent years as potential anti-infective therapeutic
67 candidates for the design of new antimicrobial agents (Craik et al., 2013; Gordon et al., 2005;
68 Parachin and Franco, 2014). In this context, isolation of new AMPs is of interest in providing general
69 insights into AMP structure and activity.

70 Marine organisms live in habitats abundant with bacteria, fungi, viruses, and parasites, some of
71 which are potentially harmful. However, many marine organisms do not seem to be vulnerable to
72 pathogenic invasions, suggesting that they have robust and effective immune effectors such as AMPs
73 to defend against microbial pathogens (Cheung et al., 2015; Falanga et al., 2016; Otero-Gonzalez et
74 al., 2010). Furthermore, AMPs from marine organisms are often taxon-specific or even species-
75 specific and are structurally different from their counterparts produced by terrestrial species (Augustin
76 et al., 2009; Charlet et al., 1996; Lee et al., 1997; Li et al., 2010b; Li et al., 2008; Smith et al., 2008).
77 Therefore, marine organisms provide fascinating sources for biochemical isolation of novel AMPs.

78 Echinoderms are a phylum of exclusively marine invertebrates that include sea star, sea urchins,
79 sand dollars, sea cucumbers, and sea lilies. As deuterostome invertebrates, they occupy an
80 intermediate phylogenetic position with respect to the vertebrates and protostome invertebrates and
81 therefore they are of particular interest from an evolutionary perspective (Blair and Hedges, 2005;
82 Smith et al., 2010). Echinoderms rely on innate immunity for defense against harmful microorganisms

83 and although they are the second largest deuterostome phylum, relatively few AMPs have been
84 isolated and characterized from these animals. Cysteine-rich AMPs (strongylocins) isolated from the
85 sea urchins *Strongylocentrotus droebachiensis*, *Strongylocentrotus purpuratus*, and *Echinus*
86 *esculentus* (Li et al., 2010a; Li et al., 2008; Solstad et al., 2016) and heterodimeric AMPs (centrocins)
87 isolated from *S. purpuratus* and *E. esculentus* (Li et al., 2010b; Solstad et al., 2016) exhibit
88 antimicrobial activity against both gram-positive and gram-negative bacteria (Li et al., 2010a; Li et
89 al., 2010b). Strongylocins and centrocins have unique structural characteristics compared to other
90 known AMPs and therefore it is of interest to identify AMPs in other echinoderms (e.g. sea star).

91 Here we report the isolation of a novel sea star cysteine-rich AMP, named *PpCrAMP*, from the
92 sea star *Patiria pectinifera*. The primary structure of *PpCrAMP* was determined by Edman
93 degradation and MALDI-TOF MS and the cysteine connectivity of four cysteine residues that form
94 two disulfide bonds in *PpCrAMP* was determined by comparison of native and synthetic peptides that
95 were produced with different combinations of two disulfide bond pairings. The antimicrobial activity
96 of synthetic *PpCrAMP* variants was showed both gram-positive and gram-negative bacteria.
97 Genomic DNA and cDNA encoding the *PpCrAMP* precursor protein were cloned and sequenced,
98 enabling investigation of its expression pattern in *P. pectinifera*. Furthermore, the organization of the
99 *PpCrAMP* gene in *P. pectinifera* was compared with homologs in other echinoderms. Discovery of
100 *PpCrAMP* is notable as it is the first cysteine-rich AMP to be purified from sea star.

101 2. Materials and Methods

102 2.1. Animals and sample collection

103 Specimens of the sea star *Patiria pectinifera* were collected at low tide from the intertidal
104 zone on the rocky coast of Cheongsapo of Busan, Korea. The sea star were immediately transferred to
105 our laboratory and maintained in a recirculating seawater system at 15 °C until sample collection. The
106 coelomic epithelium, which includes layers of longitudinal and circular muscle, was collected from
107 the aboral body wall of the arms of 100 specimens of *P. pectinifera* using sterile knives and forceps.
108 The collected sample were immediately frozen in liquid nitrogen and stored at -80 °C until extraction.
109 For immune challenge experiments, 30 live specimens of the sea star (approximate size 4-5 cm
110 determined by the distance from the center of disk to outer tip of arm) were acclimatized in a 600 L
111 recirculating aquarium tank equipped with sand-filtered and UV-sterilized seawater at 15 °C for 1
112 month. The sea star were fed once every 3 days with live manila clam, *Ruditapes philippinarum*.
113 Approval by the local institution/ethics committee was not required for this work because
114 experimental work on sea star is not subject to regulation and *P. pectinifera* is not an endangered or
115 protected species.

116 2.2. Peptide extraction and purification

117 Four volumes of 1% acetic acid was added to the frozen sample and then the mixture was
118 heated in a double boiler for 5 min to prevent proteolytic enzyme activity. The boiled sample was
119 cooled on ice and homogenized (T10 basic ULTRA-TURRAX Homogenizer system, IKA, USA). The
120 homogenate was then centrifuged (20,000 × g, 30 min, 4 °C) and then the supernatant was applied
121 onto a C18 cartridge (Sep-pak C18, 20 cc, Waters Corp, USA). The column was washed with 40 ml of
122 10% methanol/0.1% trifluoroacetic acid (TFA) and retained materials were then eluted with 40 ml of
123 60% methanol/0.1% TFA. An aliquot of the eluate was lyophilized and then dissolved in 0.01% acetic
124 acid to evaluate its antimicrobial activity against *Escherichia coli* D31 and *Bacillus subtilis*
125 KCTC1021. To purify antimicrobial components of the eluate, a portion (3 ml) of it was applied to a
126 cation-exchange column (TSKgel SP-5PW, 7.5 × 75 mm, Tosho, Japan) and eluted with a linear
127 gradient of 0 to 1.0 M sodium chloride in 10 mM phosphate buffer (PB, pH 6.0) for 100 min at a flow
128 rate of 1.0 ml/min. Absorbance peaks were monitored at 220 nm to detect peptide bonds and fractions
129 were collected manually. A bioactive peak from the first cation-exchange HPLC purification was
130 subjected to reversed phase (RP)-HPLC (Capcellpak C18, 5µm, 4.6 × 250 mm; Shisheido Co., Tokyo,
131 Japan). Elution was performed by isocratic elution in 10% acetonitrile/0.1% TFA for 10 min and then
132 a linear gradient of 10 to 60% acetonitrile/0.1% TFA for 50 min at a flow rate of 1.0 ml/min. An
133 active peak showing antimicrobial activity against *B. subtilis* KCTC 1021 was purified by

134 chromatography again using the same column as the previous step, but with isocratic elution in 22%
135 acetonitrile/0.1% TFA (peak A) at a flow rate of 1 ml/min.

136 2.3. Primary structure determination of the purified peptide

137 The molecular mass and AA sequence of the purified AMP were determined using matrix
138 assisted laser desorption/ionization (MALDI) time-of-flight (TOF) mass spectrometry (MS) with a
139 pulsed smartbeam II (355 nm Nd:YAG laser, repetition rate 1 kHz) in linear mode (Ultraflex extreme
140 from Bruker Daltonics, Billerica, MA, USA) and an automated N-terminal AA gas-phase sequencer
141 (PPSQ-31A/33A protein sequencers, Shimadzu Co., Kyoto, Japan). To confirm the existence of
142 disulfide bonds, the purified peptide was reduced with 100 µl of 0.1 M 1,4-dithiothreitol (DTT)
143 solution for 2 h at 42 °C. After reduction of disulfide bonds, the retention times of the reduced and the
144 native peptides were compared using RP-HPLC with a linear gradient of 5 - 65% acetonitrile/0.1%
145 TFA for 60 min at a flow rate of 1 ml/min.

146 2.4. Peptide synthesis and determination of disulfide bridge connectivity

147 Based on the results of structure analyses and cDNA cloning, variants of *PpCrAMP* with three
148 possible disulfide bond connectivities were custom synthesized by ChemPep Inc. (Wellington, FL,
149 USA). The synthetic peptides were re-purified to be greater than 98% pure by RP-HPLC, and
150 molecular masses were confirmed by MALDI-TOF MS. The reduced form of the synthetic peptide
151 was obtained by RP-HPLC purification followed by the same procedure used for native *PpCrAMP*.
152 The molecular mass of the reduced synthetic *PpCrAMP* was also confirmed by MALDI-TOF MS
153 with observation of a 4 mass unit difference. Identity was assessed by comparison of the retention
154 times of synthetic peptides and native *PpCrAMP* using RP-HPLC with a linear gradient of 20 to 30%
155 acetonitrile/0.1% TFA for 20 min and, then, an isocratic elution with 23% acetonitrile/0.1% TFA. The
156 quantities of the purified synthetic peptides were calculated using a linear relationship between peak
157 area and peptide amount in a serial dilution of 1 mg/ml of synthetic *PpCrAMP*.

158 2.5. Antimicrobial activity assay

159 An ultrasensitive radial diffusion assay was adopted for monitoring antimicrobial activity
160 during the purification steps and for testing synthetic peptides, as described previously (Seo et al.,
161 2016). The microbial strains used to evaluate the antimicrobial activity were *B. subtilis* KCTC1021,
162 *Staphylococcus aureus* KCTC1621, *Micrococcus luteus* KCTC1071, *E. coli* D31, *Streptococcus iniae*
163 FP5229, *Salmonella enterica* ATCC13311, *Shigella flexneri* KCTC2517, *Aeromonas hydrophila*
164 KCTC2358, *Edwardsiella tarda* NUF251, and *Vibrio parahaemolyticus* KCCM41664, and *Candida*
165 *albicans* KCTC9765 (Table 1). Briefly, microbial strains were pre-cultured overnight in tryptic soy

166 broth (TSB) at the appropriate temperatures, 25 °C for fish pathogens and 37 °C for the others. Pre-
167 cultured microbial strains were diluted with 10 mM PB (pH 6.6) to $\sim 10^8$ CFU/ml for microbial strains
168 and $\sim 10^6$ CFU/ml for the fungus *C. albicans*, and 0.5 ml of the diluted strains was mixed with 9.5 ml
169 of underlay gel containing 0.03% TSB and 1% Type I agarose in 10 mM PB (pH 6.6). Peptides were
170 serially diluted 2-fold in 5 μ l of 0.01% acetic acid and each dilution was added to 2.5 mm diameter
171 wells made in the 1 mm thick underlay gels. After 3 h of incubation at the appropriate temperatures,
172 microbial strains were overlaid with 10 ml of double-strength overlay gel containing 6% TSB with
173 10 mM PB (pH 6.6) in 1% agarose. Plates were incubated for an additional 18 - 24 h and then the
174 clear zone diameters were measured. After subtracting the diameter of the well, the clear zone
175 diameter was expressed in units (0.1 mm = 1 U). The minimal effective concentration (MEC, μ g/ml)
176 of the synthetic peptides was calculated as the X-intercept of a plot of units against the \log_{10} of the
177 peptide concentration (Lehrer et al., 1991). The antimicrobial assay was performed in triplicate and
178 the results were averaged.

179 2.6. cDNA and gene cloning

180 Cloning of a cDNA encoding the complete *PpCrAMP* precursor protein was performed by 3'
181 and 5' rapid amplification of cDNA ends (RACE) polymerase chain reaction (PCR). Total RNA was
182 extracted from the coelomic epithelium of *P. pectinifera* using Hybrid-R kit (GeneAll, Seoul, Korea),
183 and then mRNA was purified using Oligotex mRNA mini kit (Qiagen, USA) following the
184 manufacturer's instructions. The synthesis for RACE-ready cDNA template was performed with
185 GeneRacer kit (RLM-RACE, Invitrogen, CA, USA) according to the manufacturer's instructions. The
186 sequence of primers for 3'RACE was based on analysis of a GenBank transcriptome shotgun
187 assembly (TSA) database (accession no. GFOQ01277783.1) from *P. pectinifera* obtained by Illumina
188 HiSeq 2500 sequencing, reported previously by our group (Kim et al., 2017). Two sequence specific
189 primers were designed for 3' RACE, and then 5' RACE was conducted with sequence-specific
190 primers designed from the sequencing result of the 3' RACE product. The sequences of primers used
191 in RACE are listed in Table 1. The first 3'RACE reaction (30 cycles, 95 °C for 30 s, 60°C for 30 s,
192 and 72 °C for 1 min) was performed using a primer (GSP-F1) and the GeneRacer 3' primer. The PCR
193 product was re-amplified (30 cycles, 95 °C for 30 s, 58°C for 30 s, and 72 °C for 1 min) using a
194 primer (GSP-F2) and GeneRacer 3' nested primer. The 5' RACE reaction (30 cycles, 95 °C for 30 s,
195 58°C for 30 s, and 72 °C for 1 min) was completed using a gene-specific primer (GSP-R) and the
196 GeneRacer 5' primer. PCR products in the last step of 3' and 5' RACE were introduced into the
197 pGEM-Teasy vector system (Promega Corporation, USA) and sequenced. The sequence of precursor
198 transcripts obtained was submitted to the GenBank database (accession no. MF443207).

199 Based on the cDNA sequence of the *PpCrAMP* precursor, both forward (Gene F) and reverse
200 (Gene R) primers located in the 5' and 3' untranslated regions (UTRs) of the cDNA sequence were
201 designed for studying the gene structure (see Table S1 for sequences). Genomic DNA was extracted
202 from the coelomic epithelium of one animal using Exgene DNA extraction kit (GeneAll, Seoul,
203 Korea) following the manufacturer's instructions and 100 ng of genomic DNA was employed as a
204 template in PCR (30 cycles, 95 °C for 30 s, 58°C for 30 s, and 72 °C for 3 min). The PCR product
205 was also cloned into pGEM-Teasy vector and sequenced. The sequence of genomic DNA containing
206 the *PpCrAMP* gene was also submitted to the GenBank database (accession no. MF443208).

207 2.7. Real time quantitative polymerase chain reaction (RT-qPCR) of *PpCrAMP* precursor transcripts

208 RT-qPCR analysis was done to determine the basal expression level of *PpCrAMP* precursor
209 transcripts in various tissues, including coelomic epithelium, coelomocytes, gonad, oral hemal ring
210 including Tiedemann's bodies, pyloric caeca, stomach (including cardiac and pyloric regions), and
211 tube feet. Furthermore, to determine whether acute changes in the abundance of *PpCrAMP* precursor
212 transcripts occur following immune stimulation, tissues that express *PpCrAMP* constitutively
213 (coelomic epithelium and tube feet) were sampled 0, 8, 16, and 32 h post-immune stimulation. The
214 immune challenge was performed by injection with 50 µl *V. parahaemolyticus* ($OD_{600}=0.1$, 3.3×10^8
215 CFU/ml) into the coelomic cavity through the body wall at the tip of each of the arms of sea star with
216 arm lengths of 4-5 cm. Total RNA was extracted from pooled sample tissues (five individuals per
217 pool) using Hybrid-R (GeneAll, Seoul, Korea) according to the manufacturer's instructions, and RNA
218 quality was assessed by 1.0% agarose gel electrophoresis and then quantified spectrophotometrically
219 using a NanoDrop Lite (Thermo Fisher Scientific, Wilmington, MA, USA). cDNA was synthesized
220 using the TOPscript cDNA synthesis Kit with oligo dT (dT18) (Enzynomics, Deajeon, Korea)
221 according to the manufacturer's instructions. The primer pairs used for amplifying *PpCrAMP*
222 precursor cDNA and *elongation factor 1 α* (*EF1 α* , accession No. AAT06175) cDNA as a control for
223 normalization were *PpCrAMP* qPCR-F and qPCR-R, and *EF1 α* qPCR-F and qPCR-R, respectively
224 (see Table S1 for sequences). To analyze expression of *PpCrAMP* precursor transcripts in different sea
225 star tissues/organs quantitatively, RT-qPCR was employed using a CFX Connect Real-Time PCR
226 Detection System (Bio-Rad, USA), as previously described with slight modifications (Kim et al.,
227 2016). In brief, the amplification was carried out in a 20 µl reaction mixture containing 10 µl of 2 \times
228 SYBR green premix (TOPreal qPCR 2X PreMix, Enzynomics, Deajeon, Korea), 1 µl (10 pmol/µl)
229 each of forward and reverse primers, 1 µl of 10 times diluted cDNA template and nuclease free water.
230 The thermal profile was 95 °C for 10 min, 40 cycles of 95 °C for 10 s, 60 °C for 15 s and 72 °C for 15
231 s with fluorescence recording at the end of each cycle. Melt curve analysis was performed to ensure

232 product specificity over the temperature range of 60-90 °C. Amplicons were analyzed on agarose gels
233 to confirm the product size. Based on the standard curves for both *PpCrAMP* and *EF1α*, the relative
234 expression levels of *PpCrAMP* precursor transcripts in each tissue were normalized against the level
235 of the *EF1α* control using the comparative CT method ($2^{-\Delta\Delta CT}$) (Livak and Schmittgen, 2001).
236 Triplicate amplifications were carried out independently, and the results were analyzed statistically.
237 For statistical analysis of *PpCrAMP* precursor transcript expression, the graphs were generated, and
238 one-way analysis of variance (ANOVA) with Duncan's multiple range post-hoc analysis was
239 performed using GraphPad Prism software version 7.0 for Windows (GraphPad Software, San Diego,
240 California, USA). Relative fold expression was presented as means \pm standard deviation. P values
241 with $p < 0.05$ were considered statistically significant.

242 2.8. *In silico* analysis

243 A cDNA encoding the *PpCrAMP* precursor protein was translated into protein sequence using
244 Expert Protein Analysis System (ExPASy) proteomics server of the Swiss Institute of Bioinformatics
245 (<http://web.expasy.org/translate/>) and SignalP 4.1 (<http://www.cbs.dtu.dk/services/SignalP/>) was used
246 to predict the signal peptide of the translated protein sequence. Theoretical molecular mass and
247 isoelectric points of the mature *PpCrAMP* were calculated by the computer pI/Mw tools
248 (http://web.expasy.org/compute_pi/) at ExPASy. To identify potential homologs of *PpCrAMP* the
249 deduced AA sequence and genomic nucleotide sequence of the *PpCrAMP* were submitted as queries
250 for BLAST analysis of i) the NCBI/GenBank nr database (<http://blast.ncbi.nlm.nih.gov/blast.cgi>), ii)
251 the AMP database, including the collection of antimicrobial peptides (CAMP,
252 <http://www.camp.bicnirrh.res.in>), iii) the antimicrobial peptide database (APD,
253 <http://aps.unmc.edu/AP/main.php>), iv) the Echinoderm genomic database
254 (<http://www.echinobase.org/Echinobase/Blasts>) and v) neural transcriptome sequence data from the
255 sea star *Asterias rubens* (Semmens et al., 2013; Semmens et al., 2016). Multiple sequence alignment
256 of the full-length *P. pectinifera* *PpCrAMP* precursor and putative related proteins from other species
257 was performed using a multiple sequence alignment algorithm, Kalign, from the European
258 Bioinformatics Institute (EMBL-EBI) (<https://www.ebi.ac.uk/Tools/msa/kalign/>). Secondary structure
259 prediction was performed using the Network Protein Sequence Analysis (NPS@: [https://npsa-](https://npsa-prabi.ibcp.fr/)
260 [prabi.ibcp.fr/](https://npsa-prabi.ibcp.fr/)) server (Combet et al., 2000).

261 3. Results

262 3.1. Purification of AMP from the coelomic epithelium of *Patiria pectinifera*

263 An aliquot of a coelomic epithelium extract of *P. pectinifera* exhibited antimicrobial activity
264 against *B. subtilis* and *E. coli*, which was abolished by tryptic digestion (Fig. 1A), indicating that it
265 was an appropriate source to isolate AMPs. The gram-positive bacterium *B. subtilis* was highly
266 susceptible to the crude extract and so was used to test for antimicrobial activity during the
267 purification steps. A single absorbance peak (peak A) that exhibited antimicrobial activity against *B.*
268 *subtilis* was purified successfully from the coelomic epithelium extract through three steps of column
269 purification. The extract was first fractionated using cation-exchange HPLC with a salt gradient and
270 an active peak was eluted with 0.6 M sodium chloride corresponding to a retention time of 69 min
271 (Fig. 1B). The peak was further subjected to RP-HPLC and an active peak, designated as peak A, was
272 eluted with 22% acetonitrile/0.1% TFA (Fig. 1C). Finally, a single absorbance peak was obtained
273 with isocratic 22% acetonitrile/0.1% TFA elution, and this peak was then subjected to structural
274 analyses (Fig. 1D).

275 3.2. Primary structure analyses of purified AMP

276 The first 37 AAs from the N-terminus of the purified peptide were determined by Edman
277 sequencing (Fig. 2A), but with some unidentified residues (X) from blank cycles. The molecular mass
278 determined by MALDI-TOF MS was 4027.8 Da and 2014.7 as the protonated molecular ion (M+H)⁺
279 and the double charged ion (M+2H)²⁺, respectively (Fig. 2B upper panel). Without reduction and
280 alkylation cysteine residues often emerge as blank cycles during amino acid sequencing because they
281 form disulfide bonds that are important for the folding and stability of AMPs and proteins. Therefore,
282 the purified AMP from *P. pectinifera* was reduced by treatment with DTT to confirm the existence of
283 disulfide bonds. The retention time of the reduced peptide was revealed as 29.8 min, which
284 represented a delay of about 2 min compared to the native form (Fig 2C), and the molecular mass of
285 the reduced peptide was 4 Da higher than the native peptide (Fig. 2B lower panel). These data
286 indicated that the purified native peptide contained four cysteine residues that formed two
287 intramolecular disulfide bonds. Accordingly, in the deduced sequence of the AMP we replaced three
288 X residues with cysteine residues and added an additional cysteine residue at the C-terminus:
289 GRKGRKGV RGNPFFNCEDEFGNPGCVCDKRKGGAAVTC. This peptide was designated *P.*
290 *pectinifera* cysteine-rich antimicrobial peptide (*PpCrAMP*). The theoretical molecular mass of the
291 deduced peptide in reduced form was calculated as 4032.6 Da (M+H)⁺, which differed from observed
292 molecular mass of reduced *PpCrAMP* by 1 Da (Fig. 2B lower panel). C-terminal amidation is a
293 common post-translational modification of AMPs and this decreases the molecular mass by only 1 Da
294 compared to peptides with a free carboxyl-terminus. Furthermore, glycine is a substrate for C-terminal
295 amidation. To investigate if *PpCrAMP* was C-terminally amidated in this way, the AA sequence of

296 *PpCrAMP* was submitted as a query against the non-redundant protein sequences in the NCBI
297 database using BLAST (<https://blast.ncbi.nlm.nih.gov/Blast.cgi>) but no significant sequence
298 homology with other known AMPs was observed. Therefore, we attempted to find putative transcripts
299 encoding *PpCrAMP* in GenBank transcriptome shotgun assemblies (TSA) of *Patiria* (taxid: 35076)
300 using BLAST. Two transcripts were found that encoded proteins identical or similar to the AA
301 sequence of *PpCrAMP*: a 1,242 bp transcribed RNA (accession No. GFOQ01277783.1) and a 910 bp
302 transcribed RNA (accession No. GAWB01039446.1) from *de novo* assembled transcriptomes of *P.*
303 *pectinifera* and *P. miniata*, respectively (Fig. 2D). The transcripts encoded *PpCrAMP* or a *PpCrAMP*-
304 like protein with a glycine residue at its C-terminus, consistent with this residue being a substrate for
305 amidation mediated by peptidylglycine α -amidating monooxygenase (PAM) (Eipper et al., 1991) and
306 the mature *PpCrAMP* peptide having an α -amide at the C-terminus. In conclusion, the structural
307 analyses demonstrated that *PpCrAMP* was a C-terminally amidated cationic AMP (with a predicted
308 isoelectric point (pI) of 9.20; http://web.expasy.org/compute_pi/) comprising 38 AAs, which include
309 four cysteine residues (Cys¹⁶, Cys²⁵, Cys²⁷ and Cys³⁸) that form two disulfide bonds (Fig. 2D).

310 3.3. Determination of cysteine connectivity in native *PpCrAMP*

311 The four cysteine residues in *PpCrAMP* could mediate three different cysteine connectivities to
312 form two intramolecular disulfide bonds. To determine the authentic cysteine connectivity in the
313 native peptide, we synthesized C-terminally amidated *PpCrAMP*s that have the three different
314 cysteine connectivities: *PpCrAMP*-1 (Cys¹⁶-Cys²⁵ and Cys²⁷-Cys³⁸), *PpCrAMP*-2 (Cys¹⁶-Cys²⁷ and
315 Cys²⁵-Cys³⁸) and *PpCrAMP*-3 (Cys¹⁶-Cys³⁸ and Cys²⁵-Cys²⁷) corresponding to C1-C2 and C3-C4,
316 C1-C3 and C2-C4, and C1-C4 and C2-C3, respectively (Fig. 3A). The retention time of native
317 *PpCrAMP* was compared with the elution times of the synthetic peptides using RP-HPLC. Native
318 *PpCrAMP* was eluted at 15.1 min in a gradient elution, which was almost identical to the retention
319 time (14.9 min) of synthetic *PpCrAMP*-2. In contrast, both synthetic *PpCrAMP*-1 and *PpCrAMP*-3
320 and the reduced form of *PpCrAMP* (*PpCrAMP*_{reduced}) were eluted at 16.6, 16.8 and 19.1 min on the
321 same RP-HPLC, respectively, which represented delays of 2 to 4 min compared to the native peptide
322 (Fig. 3B). Furthermore, native *PpCrAMP* and synthetic *PpCrAMP*-2 co-eluted with isocratic RP-
323 HPLC (Fig. 3C), whereas the retention times of both synthetic *PpCrAMP*-1 and *PpCrAMP*-3 were
324 not identical to synthetic *PpCrAMP*-2 (Fig. 3D and E). Collectively, these findings indicated that the
325 four cysteine residues in native *PpCrAMP* formed two disulfide bonds with Cys¹⁶-Cys²⁷ and Cys²⁵-
326 Cys³⁸ pairings (i.e. C1-C3, C2-C4 connectivity) and the C-terminus of native *PpCrAMP* was
327 amidated.

328 3.4. Antimicrobial activity of synthetic *PpCrAMP* variants

329 All four synthetic *PpCrAMP* variants exhibited antimicrobial activity against the gram-negative
330 bacteria *S. enterica* and *S. flexneri*, with a minimal effective concentration (MEC) of 4.5 to
331 31.4 µg/ml, and against the gram-positive bacteria *B. subtilis*, *S. aureus*, and *M. luteus*, with a MEC of
332 15.6 to >250 µg/ml. However, the antimicrobial activity of synthetic *PpCrAMP*-2 was significantly
333 higher than the antimicrobial activity of the other synthetic *PpCrAMP*s and reduced *PpCrAMP* (Table
334 1). The most potent antimicrobial activity exhibited by all four synthetic *PpCrAMP*s was against the
335 gram-negative bacterium *S. enterica* [MECs, 4.5 – 8.4 µg/ml]. However, antimicrobial activity of
336 synthetic *PpCrAMP*s was barely detectable against fish pathogens and was undetectable with the
337 fungus *C. albicans*. These findings demonstrated that the existence of the disulfide bonds in
338 *PpCrAMP* was not critical for antimicrobial activity, but the cysteine connectivity in native *PpCrAMP*
339 corresponding to C1-C3 and C2-C4 was required for maximum activity against the bacteria tested
340 here. Interestingly, while coelomic epithelium extract showed antimicrobial activity against *E. coli*
341 D31 (Fig. 1A), all four synthetic *PpCrAMP*s did not show antimicrobial activity against *E. coli* D31
342 up to a peptide concentration of 250 µg/ml, indicating that the coelomic epithelium extract also
343 contained other AMPs responsible for antimicrobial activity against *E. coli* D31.

344 3.5. cDNA and genomic DNA sequence encoding *PpCrAMP*

345 To obtain the complete sequence of the *PpCrAMP* precursor protein, a cDNA encoding
346 *PpCrAMP* was cloned and sequenced (accession number: MF443207). The cDNA of the *PpCrAMP*
347 precursor comprised 926 bp, starting with a 5'-UTR of 81 bp, followed by an open reading frame
348 (ORF) of 240 bp, a 3'-UTR of 605 bp containing a polyadenylation consensus sequence (AATAAA)
349 located at 31 bp upstream of a poly(A)⁺ tail (Fig. 4A). The deduced AA sequence of the ORF of the
350 *PpCrAMP* precursor started with a signal peptide of 21 residues, as predicted by SignalP 4.1,
351 followed by two peptide fragments cleaved at putative dibasic cleavage site (Lys³⁹Arg⁴⁰): an N-
352 terminal prosequence (Ser²²-Val³⁸) containing several anionic AAs and mature *PpCrAMP* consisting
353 of 38 AAs plus one C-terminal glycine residue (Gly⁴¹-Gly⁷⁹), consistent with the structural analyses
354 (Fig. 4B). Accordingly, these sequence data demonstrated that *PpCrAMP* was derived from a larger
355 precursor protein which underwent post-translational modifications such as formation of disulfide
356 bonds and α-amidation at the C-terminus followed by cleavage at a putative dibasic cleavage site
357 (KR) between the anionic prosequence and the mature peptide. The genomic DNA sequence encoding
358 *PpCrAMP* (accession number: MF443208) comprised two exons and one intron (Fig. 4B). The first
359 exon comprised a 5' UTR followed by an ORF encoding the signal peptide, the prosequence, and the
360 first 14 AAs of mature *PpCrAMP*, which was followed by an 896 bp intron. The second exon
361 comprised an ORF encoding the cysteine-rich region of *PpCrAMP* (25 AAs) followed by a 3' UTR.

362 The classical canonical splicing recognition sequence GT/AG was present at the exon-intron
363 junctions.

364 BLAST analysis revealed that *PpCrAMP* exhibited no significant sequence homology with other
365 known AMP precursors. However, genomic DNA sequence encoding *PpCrAMP* exhibited sequence
366 similarity with genes in the sea star *P. miniata* (accession No. AKZP01101613), the sea star
367 *Acanthaster planci* (accession No. BDGH01001773), the sea cucumber *P. parvimensis* (accession No.
368 JXUT0100825), and the sea urchin *S. purpuratus* (accession No. AAGJ05078965) (Fig. 5A). All four
369 genes were similar to the *P. pectinifera PpCrAMP* gene in containing one intron and two exons, which
370 encoded homologs of the *PpCrAMP* precursor. In addition, analysis of neural transcriptome sequence
371 data from the sea star *Asterias rubens* (Semmens et al., 2013; Semmens et al., 2016) revealed two
372 transcripts encoding homologs of the *PpCrAMP* precursor – *ArCrAMP-1* precursor (accession
373 number: MG711458) and *ArCrAMP-2* precursor (accession number: MG711459). A multiple
374 alignment of the *PpCrAMP* precursor with homologs identified in other echinoderms is shown in Fig.
375 5B. The *PpCrAMP* precursor shared 96.2% AA identity with the homolog from the sea star *P.*
376 *miniata*, 53.6% AA identity with the homolog from the sea star *A. planci*, 45.7% and 46.6% identity
377 with the two homologs from the sea star *A. rubens*, 43.1% AA identity with the homolog from the sea
378 urchin *S. purpuratus*, and 34.3% AA with the homolog from the sea cucumber *P. parvimensis*.
379 Collectively, these data indicated that *PpCrAMP* was the prototype for a novel family of cysteine-rich
380 AMPs that occur in echinoderms.

381

382 3.6. RT-qPCR analysis for *PpCrAMP* mRNA

383 To compare expression levels of *PpCrAMP* transcript in various sea star tissues and post immune
384 challenge, the relative expression levels of the *PpCrAMP* precursor transcript in different tissues
385 (coelomic epithelium, coelomocytes, gonad, oral hemal ring, pyloric caeca, stomach, and tube feet) of
386 *P. pectinifera* were determined by RT-qPCR using sequence specific primers targeting the *PpCrAMP*
387 coding region. An *EF1 α* gene was used as an invariant control and for comparison of relative
388 expression between transcripts (Kim et al., 2016). The results showed that the highest expression level
389 of *PpCrAMP* precursor transcripts was detected in the tube feet and the coelomic epithelium, which
390 was the original source of *PpCrAMP* in this study, followed by moderate expression levels in the oral
391 hemal ring (including Tiedemann's bodies), and the stomach (Fig. 6A). These findings indicated that
392 the coelomic epithelium and the tube feet were the major tissues/organs that produced *PpCrAMP* in *P.*
393 *pectinifera*. Accordingly, these two tissues were selected to determine whether acute changes in the
394 abundance of *PpCrAMP* precursor transcript occur after bacterial challenge. However, no significant

395 changes in *PpCrAMP* precursor expression were observed at different times after the bacterial
396 challenge (Fig. 6B).
397

398 **4. Discussion**

399 Few AMPs have been identified in echinoderms to date. Strongylocins and centrocins were first
400 isolated from coelomocytes of the green sea urchin (*S. droebachiensis*) and related peptides
401 (SpStrongylocins 1 and 2) were then discovered and characterized in the purple sea urchin
402 (*S. purpuratus*) and the edible sea urchin (*E. esculentus*) (Li et al., 2010a; Li et al., 2010b; Li et al.,
403 2008; Solstad et al., 2016). These are cationic peptides that exhibit antimicrobial activity against both
404 gram-positive and gram-negative bacteria (Li et al., 2010a; Li et al., 2008). Strongylocins with six
405 cysteine residues forming three intramolecular disulfide bonds show a cysteine arrangement pattern
406 different from any known cysteine-rich AMPs with six cysteine residues and have post-translational
407 modifications such as a brominated tryptophan (Li et al., 2008). Centrocins have a heterodimeric
408 structure, containing a heavy chain (30 AAs) and a light chain (12 AAs), and also have a brominated
409 tryptophan (Li et al., 2010b). Thus, AMPs isolated from echinoderm species, including strongylocins
410 and centrocins, have distinct structures compared to those that have been isolated from vertebrates and
411 protostomes. Here we report the purification from an extract of the coeleomic epithelium of the sea
412 star *P. pectinifera* of a novel AMP designated *PpCrAMP*, which contains four cysteine residues that
413 form two disulfide bonds and which has a amidated C-terminal cysteine (Fig. 2 and 3).

414 Cysteine-rich AMPs represent the most diverse and widely distributed family of AMPs in the
415 animal kingdom. Depending on the number of cysteine residues (mostly between 2 to 8) and their
416 pairing, cysteine-rich AMPs are classified into three groups: a β -sheet conformation with triple strands,
417 a β -hairpin-like structure, and a mixed α -helix/ β -sheet conformation (Bulet et al., 2004). Among these
418 three groups of peptides, AMPs containing four cysteine residues that form two disulfide bonds have
419 been identified in arthropods and pigs (Fig. 7): tachypleisin and polypemusins from the horseshoe crab
420 *Tachypleus tridentatus* and *Limulus polyphemus* (Miyata et al., 1989; Nakamura et al., 1988),
421 respectively, gomesin from the spider *Acanthoscuria gomesiana* (Silva et al., 2000), androctonin from
422 the scorpion *Androctonus australis* (Ehret-Sabatier et al., 1996), and protegrin from porcine
423 leukocytes (Storici and Zanetti, 1993). Moreover, with exception of androctonin, all of these peptides
424 are amidated at the C-terminus and their cysteine connectivity is C1-C4 and C2-C3 (Fahrner et al.,
425 1996; Laederach et al., 2002; Mandard et al., 2002). In contrast, the novel AMP identified here in the
426 sea star *P. pectinifera*, *PpCrAMP*, has two disulfide bonds with C1-C3 and C2-C4 connectivity.

427 The antimicrobial activity of synthetic *PpCrAMP*, with C1-C3 and C2-C4 cysteine connectivity
428 (*PpCrAMP*-2), is identical to that of the native peptide, and synthetic *PpCrAMP*-2 exhibits the most
429 potent activity against both gram-positive and gram-negative bacteria compared with other synthetic
430 variants. Investigation of the importance of the disulfide bonds in cysteine-rich antimicrobial peptides

431 with two disulfide bonds demonstrates that the peptides require the correct disulfide bond
432 configuration to adopt a conformation such as the β -hairpin-like structure and to retain full bioactivity
433 (Laederach et al., 2002; Mani et al., 2005; Muhle and Tam, 2001; Rao, 1999). The β -hairpin-like
434 structure consists of two antiparallel β -strands stabilized by a disulfide bond, linked by a short loop of
435 two to five amino acids (Panteleev et al., 2015). The β -hairpin-like structure that is essential for the
436 activity seen in cysteine-rich AMPs (e.g. tachyplesin-I and protegrin-I) is consistent with the predicted
437 consensus secondary structure of *PpCrAMP* (Fig. 7). Analysis of the sequence of *PpCrAMP* using the
438 NPS@ server indicates that *PpCrAMP* is likely to adopt a β -hairpin-like structure consisting of two
439 extended β -strands (residues 25-28 and 35-37) linked by a random coil region. Therefore, the potent
440 antimicrobial activity of synthetic *PpCrAMP-2* may reflect the disulfide bond connectivity that
441 establishes the most stable structure. Further investigation of the relationship between conformation
442 and antimicrobial activity of *PpCrAMP* will be required to address this issue. Homologs of *PpCrAMP*
443 identified in other echinoderms also have four cysteine residues in equivalent positions but C-terminal
444 amidation appears not to be a generic characteristic. For example, the two *PpCrAMP*-type proteins
445 identified in the sea star *A. rubens* do not have C-terminal glycine residue that could provide a
446 substrate for C-terminal amidation.

447 The *PpCrAMP* gene contains an intron that interrupts the region of the open reading frame
448 encoding the mature *PpCrAMP*, with one exon encoding the N-terminal domain and another exon
449 encoding the C-terminal domain that contains four cysteine residues. Orthologous genes in other
450 echinoderm species, including the sea cucumber *P. parvimensis* and the sea urchin *S. purpuratus*,
451 have the same intron/exon structure (Fig. 4 and 5). Although the organization of genes encoding
452 cysteine-rich AMPs is very diverse, the peptides are classified in the same structural scaffold group
453 based upon size, cysteine pattern and function, revealing links between the AMPs found in vertebrates
454 and those found in invertebrates (Charlet et al., 1996; Froy, 2005). Nothing is known about the
455 occurrence of *PpCrAMP*-like proteins in other phyla. However, the occurrence of *PpCrAMP*-type
456 proteins in echinoderms, a phylum that occupies an “intermediate” position with respect to the
457 deuterostome invertebrates, which include two chordate subphyla that are closely related to
458 vertebrates and the Ambulacraria, and protostome invertebrates, indicates there is a possibility of the
459 presence of orthologous genes and proteins related to defense in deuterostome invertebrates as well as
460 protostomes.

461 Analysis of the expression of the *PpCrAMP* precursor transcripts in *P. pectinifera* using qPCR
462 reveals that the coelomic epithelium and the tube feet are a major source of *PpCrAMP*. This is
463 consistent with our recent finding that the coelomic epithelium and the tube feet are grouped in a

464 tissue/organ cluster with a related biological functions based on an evaluation of differentially
465 expressed genes in *P. pectinifera* using *de novo* transcriptome data (BioProject accession:
466 PRJNA371229) (Kim et al., 2017). The coelomic epithelium is a tissue layer that lines the aboral
467 inner surface of the body wall of sea star. It appears to be a unique tissue with many features of an
468 “ancient multifunctional organogenetic tissue”, which is involved not only in common epithelial
469 functions, but also in a range of important biological processes such as wound healing, regeneration,
470 and haematopoiesis (Bossche and Jangoux, 1976; Holm et al., 2008). The absence of change in the
471 expression levels of the *PpCrAMP* precursor transcripts after immune challenge suggests that
472 *PpCrAMP* may contribute to innate immune defense in an indirect manner. Recent study on the
473 neuropeptide NDA-1, which was secreted in sensory and ganglion of the ectodermal epithelium of the
474 model organism *Hydra* during early development, surprisingly shows antimicrobial activity that may
475 affect microbiome composition on the body surface (Augustin et al., 2017). *PpCrAMP* may also
476 contribute to endocrine system with antimicrobial activity in a similar manner on the body surface.

477 In conclusion, *PpCrAMP*, the cysteine-rich AMP isolated from the coelomic epithelium of the
478 sea star *P. pectinifera*, is the first reported sea star AMP. This study increases our knowledge of AMPs
479 that are involved in the innate immune system of sea star and other echinoderm species and may lead
480 to the discovery of homologs that are involved in immune mechanisms of other animal types.
481 Furthermore, *PpCrAMP* along with AMPs isolated from other echinoderms may provide a framework
482 for development of novel antimicrobial drugs.

483 **Acknowledgements**

484 The research was supported by the Korea Ministry of Environment (MOE) “Eco-innovation Program
485 (201300030002)”

486

487 **5. References**

- 488 Augustin, R., Anton-Erxleben, F., Jungnickel, S., Hemmrich, G., Spudy, B., Podschun, R., Bosch,
489 T.C., 2009. Activity of the novel peptide arminin against multiresistant human pathogens shows
490 the considerable potential of phylogenetically ancient organisms as drug sources. *Antimicrob.*
491 *Agents Chemother.* 53, 5245-5250.
- 492 Augustin, R., Schröder, K., Murillo Rincón, A.P., Fraune, S., Anton-Erxleben, F., Herbst, E.M.,
493 Wittlieb, J., Schwentner, M., Grötzinger, J., Wassenaar, T.M. and Bosch, T.C.G. 2017. A secreted
494 antibacterial neuropeptide shapes the microbiome of *Hydra*. *Nat. Commun.* 8, 698.
- 495 Blair, J.E., Hedges, S.B., 2005. Molecular phylogeny and divergence times of deuterostome animals.
496 *Mol. Biol. Evol.* 22, 2275-2284.
- 497 Bossche, J.P., Jangoux, M., 1976. Epithelial origin of starfish coelomocytes. *Nature* 261, 227-228.
- 498 Bowdish, D.M., Davidson, D.J., Scott, M.G., Hancock, R.E., 2005. Immunomodulatory activities of
499 small host defense peptides. *Antimicrob. Agents Chemother.* 49, 1727-1732.

500 Bulet, P., Stocklin, R., Menin, L., 2004. Anti-microbial peptides: from invertebrates to vertebrates.
501 Immunol. Rev. 198, 169-184.

502 Charlet, M., Chernysh, S., Philippe, H., Hetru, C., Hoffmann, J.A., Bulet, P., 1996. Innate immunity.
503 Isolation of several cysteine-rich antimicrobial peptides from the blood of a mollusc, *Mytilus*
504 *edulis*. J. Biol. Chem. 271, 21808-21813.

505 Cheung, R.C., Ng, T.B., Wong, J.H., 2015. Marine Peptides: Bioactivities and Applications. Mar.
506 Drugs 13, 4006-4043.

507 Combet, C., Blanchet, C., Geourjon, C., Deleage, G., 2000. NPS@: network protein sequence
508 analysis. Trends Biochem. Sci. 25, 147-150.

509 Craik, D.J., Fairlie, D.P., Liras, S., Price, D., 2013. The future of peptide-based drugs. Chem. Biol.
510 Drug Des. 81, 136-147.

511 Ehret-Sabatier, L., Loew, D., Goyffon, M., Fehlbaum, P., Hoffmann, J.A., van Dorsselaer, A., Bulet,
512 P., 1996. Characterization of novel cysteine-rich antimicrobial peptides from scorpion blood. J.
513 Biol. Chem. 271, 29537-29544.

514 Eipper, B.A., Perkins, S.N., Husten, E.J., Johnson, R.C., Keutmann, H.T., Mains, R.E., 1991.
515 Peptidyl-alpha-hydroxyglycine alpha-amidating lyase. Purification, characterization, and
516 expression. J. Biol. Chem. 266, 7827-7833.

517 Fahrner, R.L., Dieckmann, T., Harwig, S.S., Lehrer, R.I., Eisenberg, D., Feigon, J., 1996. Solution
518 structure of protegrin-1, a broad-spectrum antimicrobial peptide from porcine leukocytes. Chem.
519 Biol. 3, 543-550.

520 Falanga, A., Lombardi, L., Franci, G., Vitiello, M., Iovene, M.R., Morelli, G., Galdiero, M., Galdiero,
521 S., 2016. Marine antimicrobial peptides: nature provides templates for the design of novel
522 compounds against pathogenic bacteria. Int. J. Mol. Sci. 17.

523 Froy, O., 2005. Convergent evolution of invertebrate defensins and nematode antibacterial factors.
524 Trends Microbiol. 13, 314-319.

525 Ganz, T., 2003. The role of antimicrobial peptides in innate immunity. Integr. Comp. Biol. 43, 300-
526 304.

527 Gordon, Y.J., Romanowski, E.G., McDermott, A.M., 2005. A review of antimicrobial peptides and
528 their therapeutic potential as anti-infective drugs. Curr. Eye Res. 30, 505-515.

529 Guilhelmelli, F., Vilela, N., Albuquerque, P., Derengowski Lda, S., Silva-Pereira, I., Kyaw, C.M.,
530 2013. Antibiotic development challenges: the various mechanisms of action of antimicrobial
531 peptides and of bacterial resistance. Front. Microbiol. 4, 353.

532 Hancock, R.E., Lehrer, R., 1998. Cationic peptides: a new source of antibiotics. Trends Biotechnol.
533 16, 82-88.

534 Hancock, R.E., Sahl, H.G., 2006. Antimicrobial and host-defense peptides as new anti-infective
535 therapeutic strategies. Nat. Biotechnol. 24, 1551-1557.

536 Holm, K., Dupont, S., Skold, H., Stenius, A., Thorndyke, M., Hernroth, B., 2008. Induced cell
537 proliferation in putative haematopoietic tissues of the sea star, *Asterias rubens* (L.). J. Exp. Biol.
538 211, 2551-2558.

539 Kim, C.H., Go, H.J., Oh, H.Y., Jo, Y.H., Elphick, M.R., Park, N.G., 2017. Transcriptomics reveals
540 tissue/organ-specific differences in gene expression in the starfish *Patiria pectinifera*. Mar
541 Genom. 37, 92-96.

542 Kim, C.H., Kim, E.J., Go, H.J., Oh, H.Y., Lin, M., Elphick, M.R., Park, N.G., 2016. Identification of a
543 novel starfish neuropeptide that acts as a muscle relaxant. J. Neurochem. 137, 33-45.

544 Laederach, A., Andreotti, A.H., Fulton, D.B., 2002. Solution and micelle-bound structures of
545 tachyplesin I and its active aromatic linear derivatives. Biochem. 41, 12359-12368.

546 Lee, I.H., Cho, Y., Lehrer, R.I., 1997. Styelins, broad-spectrum antimicrobial peptides from the
547 solitary tunicate, *Styela clava*. Comp. Biochem. Physiol. B, Biochem. Mol. Biol. 118, 515-521.

548 Lehrer, R.I., Rosenman, M., Harwig, S.S., Jackson, R., Eisenhauer, P., 1991. Ultrasensitive assays for
549 endogenous antimicrobial polypeptides. J. Immunol. Methods 137, 167-173.

550 Li, C., Blencke, H.-M., Smith, L.C., Karp, M.T., Stensvåg, K., 2010a. Two recombinant peptides,
551 SpStrongylocins 1 and 2, from *Strongylocentrotus purpuratus*, show antimicrobial activity
552 against Gram-positive and Gram-negative bacteria. *Dev. Comp. Immunol.* 34, 286-292.

553 Li, C., Haug, T., Moe, M.K., Styrvold, O.B., Stensvåg, K., 2010b. Centrocins: isolation and
554 characterization of novel dimeric antimicrobial peptides from the green sea urchin,
555 *Strongylocentrotus droebachiensis*. *Dev. Comp. Immunol.* 34, 959-968.

556 Li, C., Haug, T., Styrvold, O.B., Jørgensen, T.Ø., Stensvåg, K., 2008. Strongylocins, novel
557 antimicrobial peptides from the green sea urchin, *Strongylocentrotus droebachiensis*. *Dev. Comp.*
558 *Immunol.* 32, 1430-1440.

559 Liu, L., Ganz, T., 1995. The pro region of human neutrophil defensin contains a motif that is essential
560 for normal subcellular sorting. *Blood* 85, 1095-1103.

561 Livak, K.J., Schmittgen, T.D., 2001. Analysis of relative gene expression data using real-time
562 quantitative PCR and the 2^{-Delta Delta C(T)} Method. *Methods (San Diego, Calif.)* 25, 402-
563 408.

564 Mandard, N., Bulet, P., Caille, A., Daffre, S., Vovelle, F., 2002. The solution structure of gomesin, an
565 antimicrobial cysteine-rich peptide from the spider. *Eur. J. Biochem.* 269, 1190-1198.

566 Mani, R., Waring, A.J., Lehrer, R.I., Hong, M., 2005. Membrane-disruptive abilities of β -hairpin
567 antimicrobial peptides correlate with conformation and activity: A 31P and 1H NMR study.
568 *Biochim.Biophys. Acta* 1716, 11-18.

569 Miyata, T., Tokunaga, F., Yoneya, T., Yoshikawa, K., Iwanaga, S., Niwa, M., Takao, T., Shimonishi,
570 Y., 1989. Antimicrobial peptides, isolated from horseshoe crab hemocytes, tachyplesin II, and
571 polyphemusins I and II: chemical structures and biological activity. *J. Biochem.* 106, 663-668.

572 Muhle, S.A., Tam, J.P., 2001. Design of Gram-negative selective antimicrobial peptides. *Biochem.* 40,
573 5777-5785.

574 Nakamura, T., Furunaka, H., Miyata, T., Tokunaga, F., Muta, T., Iwanaga, S., Niwa, M., Takao, T.,
575 Shimonishi, Y., 1988. Tachyplesin, a class of antimicrobial peptide from the hemocytes of the
576 horseshoe crab (*Tachypleus tridentatus*). Isolation and chemical structure. *J. Biol. Chem.* 263,
577 16709-16713.

578 Oppenheim, J.J., Yang, D., 2005. Alarmins: chemotactic activators of immune responses. *Curr. Opin.*
579 *Immunol.* 17, 359-365.

580 Otero-Gonzalez, A.J., Magalhaes, B.S., Garcia-Villarino, M., Lopez-Abarrategui, C., Sousa, D.A.,
581 Dias, S.C., Franco, O.L., 2010. Antimicrobial peptides from marine invertebrates as a new
582 frontier for microbial infection control. *FASEB J.* 24, 1320-1334.

583 Pantelev, P.V., Bolosov, I.A., Balandin, S.V., Ovchinnikova, T.V., 2015. Structure and biological
584 functions of β -hairpin antimicrobial peptides. *Acta Naturae* 7, 37-47.

585 Parachin, N.S., Franco, O.L., 2014. New edge of antibiotic development: antimicrobial peptides and
586 corresponding resistance. *Front. Microbiol.* 5, 147.

587 Rao, A.G., 1999. Conformation and antimicrobial activity of linear derivatives of tachyplesin lacking
588 disulfide bonds. *Arch. Biochem. Biophys.* 361, 127-134.

589 Semmens, D.C., Dane, R.E., Pancholi, M.R., Slade, S.E., Scrivens, J.H., Elphick, M.R., 2013.
590 Discovery of a novel neurophysin-associated neuropeptide that triggers cardiac stomach
591 contraction and retraction in starfish. *J. Exp. Biol.* 216, 4047-4053.

592 Semmens, D.C., Mirabeau, O., Moghul, I., Pancholi, M.R., Wurm, Y., Elphick, M.R., 2016.
593 Transcriptomic identification of starfish neuropeptide precursors yields new insights into
594 neuropeptide evolution. *Open Biol.* 6, 150224.

595 Seo, J.K., Go, H.J., Kim, C.H., Nam, B.H., Park, N.G., 2016. Antimicrobial peptide, hdMolluscidin,
596 purified from the gill of the abalone, *Haliotis discus*. *Fish Shellfish Immunol.* 52, 289-297.

597 Silva, P.I., Jr., Daffre, S., Bulet, P., 2000. Isolation and characterization of gomesin, an 18-residue
598 cysteine-rich defense peptide from the spider *Acanthoscurria gomesiana* hemocytes with
599 sequence similarities to horseshoe crab antimicrobial peptides of the tachyplesin family. *J. Biol.*
600 *Chem.* 275, 33464-33470.

601 Smith, L.C., Ghosh, J., Buckley, K.M., Clow, L.A., Dheilly, N.M., Haug, T., Henson, J.H., Li, C.,
602 Lun, C.M., Majeske, A.J., Matranga, V., Nair, S.V., Rast, J.P., Raftos, D.A., Roth, M., Sacchi, S.,
603 Schrankel, C.S., Stensvag, K., 2010. Echinoderm immunity. *Adv. Exp. Med. Biol.* 708, 260-301.
604 Smith, V.J., Fernandes, J.M., Kemp, G.D., Hauton, C., 2008. Crustins: enigmatic WAP domain-
605 containing antibacterial proteins from crustaceans. *Dev. Comp. Immunol.* 32, 758-772.
606 Solstad, R.G., Li, C., Isaksson, J., Johansen, J., Svenson, J., Stensvag, K., Haug, T., 2016. Novel
607 antimicrobial peptides EeCentrocins 1, 2 and EeStrongylocin 2 from the edible sea urchin
608 *Echinus esculentus* have 6-Br-Trp post-translational modifications. *PLoS ONE* 11, e0151820.
609 Sperstad, S.V., Haug, T., Blencke, H.M., Styrvold, O.B., Li, C., Stensvag, K., 2011. Antimicrobial
610 peptides from marine invertebrates: challenges and perspectives in marine antimicrobial peptide
611 discovery. *Biotechnol. Adv.* 29, 519-530.
612 Storici, P., Zanetti, M., 1993. A novel cDNA sequence encoding a pig leukocyte antimicrobial peptide
613 with a cathelin-like pro-sequence. *Biochem. Biophys. Res. Commun.* 196, 1363-1368.
614 Valore, E.V., Ganz, T., 1992. Posttranslational processing of defensins in immature human myeloid
615 cells. *Blood* 79, 1538-1544.
616 Wang, G., Li, X., Wang, Z., 2016. APD3: the antimicrobial peptide database as a tool for research and
617 education. *Nucleic Acids Res.* 44, D1087-1093.
618 Zasloff, M., 2002. Antimicrobial peptides of multicellular organisms. *Nature* 415, 389-395.

619 **Figure legends**

620 **Fig. 1.** Isolation of an AMP from an extract of coelomic epithelium of the sea star *P. pectinifera*. (A)
621 Antimicrobial activity of the crude and the trypsin treated extract against *B. subtilis* KCTC 1021 and
622 *E. coli* D31 is shown. (B) Fractionation of the crude extract by cation-exchange HPLC reveals an
623 active peak (downward arrow) is eluted with 0.6 M sodium chloride. (C). A single absorbance peak
624 (peak A) responsible for the antimicrobial activity against *B. subtilis* was obtained in the second RP-
625 HPLC step. (D) Peak A was isolated through RP-HPLC with isocratic elution in 22%
626 acetonitrile/0.1% TFA.

627 **Fig. 2.** Primary structure determination of purified AMP. (A) N-terminal 37 amino acid residues of
628 purified peak A was determined by Edman degradation. (B) The retention times of the native peptide
629 and the reduced peptide (after treatment 0.1 M DTT) on RP-HPLC were compared. (C). MALDI-TOF
630 MS analysis of the native peptide and the reduced peptide showed a 4 Da difference in molecular
631 mass consistent with the presence of two disulfide bonds. (D). Complete primary structure of purified
632 peak A designated *P. pectinifera* cysteine-rich AMP (*PpCrAMP*) comprised 38 AAs with C-terminal
633 α -amidation and was compared with sequences derived from transcriptome data obtained from *P.*
634 *pectinifera* and *P. miniata*.

635 **Fig. 3.** Determination of the disulfide bond cysteine connectivity of native *PpCrAMP* (A) Structures
636 of four *PpCrAMP* variants with three different disulfide bond connectivities or without disulfide
637 bonds are shown. (B) The retention times of native *PpCrAMP* and synthetic variants were compared
638 using RP-HPLC with a linear gradient of 20% to 30% acetonitrile/0.1% TFA over 20 min. (C) Native
639 *PpCrAMP* co-elutes with synthetic *PpCrAMP* that has a C1-C3 and C2-C4 connectivity using RP-
640 HPLC under isocratic conditions with 23% acetonitrile/0.1% TFA. (D) Synthetic *PpCrAMP*-1 and
641 *PpCrAMP*-3 co-elute under the same conditions as in (C). (E) Synthetic *PpCrAMP*-1 and *PpCrAMP*-
642 2 do not co-elute under the same conditions as in (C).

643 **Fig. 4.** Sequence and structural features of the *P. pectinifera* *PpCrAMP* precursor. (A) Schematic
644 showing the structure of a cDNA encoding the *PpCrAMP* precursor protein is shown. (B) DNA
645 sequence of the gene encoding the *PpCrAMP* precursor protein, which comprises two exons (upper
646 case) separated by an intron (lowercase) is shown. The canonical splicing recognition sequence
647 GT/AG and the polyadenylation signal site are shadow boxed and underlined, respectively. The amino
648 acid sequence of the precursor is shown below the coding sequence, with the predicted signal peptide,
649 anionic prosequence and purified mature *PpCrAMP* shown in blue, black, and red, respectively, and a
650 putative dibasic cleavage site (KR) shown in green. A glycine residue that provides a substrate for C-
651 terminal amidation is boxed and the stop codon is indicated with an asterisk. The sequences of the

652 cDNA and genomic DNA encoding the *PpCrAMP* precursor are accessible from GenBank under
653 accession numbers MF443207 and MF443208, respectively.

654 **Fig. 5.** Comparison of the gene structure and sequences of *PpCrAMP*-type proteins in echinoderms
655 (A). The structure of the gene encoding *PpCrAMP* in the sea star *P. pectinifera* with related genes in
656 the sea star *P. miniata* and *A. planci*, the sea cucumber *P. parvimensis*, and the sea urchin *S* are
657 compared. *purpuratus*: (B) Sequence alignment of *P. pectinifera PpCrAMP* with *PpCrAMP*-like
658 peptides from other echinoderms.

659 **Fig. 6.** Quantitative analysis of basal expression of *PpCrAMP* precursor transcripts in various
660 organs/tissues (A) and after immune challenge in the coelomic epithelium and the tube feet (B) from
661 *P. pectinifera*. The relative expression levels of *PpCrAMP* transcripts in each organ/tissue were
662 normalized against the level of the *EF1 α* gene as an internal control. Means \pm standard deviation
663 ($n=3$) are shown. Means denoted by the same letter did not differ significantly ($p > 0.05$) while
664 different letters (a, b, c, d) at the top of the bars indicate statistically significant differences ($p < 0.05$)
665 between tissues determined by one-way ANOVA followed by Duncan's Multiple Range test.

666 **Fig. 7.** Comparison of amino acid sequence and cysteine array of *P. pectinifera PpCrAMP* to
667 vertebrate and invertebrate cysteine-rich AMPs that have four cysteine residues forming two disulfide
668 bonds and adopting β -hairpin-like structure. *PpCrAMP* is compared with (i) tachyplesin-I and (ii)
669 polyphemusin-I from the horseshoe crabs *T. tridentatus* and *L. polyphemus*, respectively (Miyata et
670 al., 1989; Nakamura et al., 1988); (iii) gomesin from the spider *A. gomesiana* (Silva et al., 2000); (iv)
671 androctonin from the scorpion *A. australis* (Ehret-Sabatier et al., 1996); (v) protegrin from from
672 porcine leukocytes (Storici and Zanetti, 1993). Lowercase (a) at the C-terminus of peptides and
673 lowercase (p) at the N-terminus of peptides indicate a C-terminal α -amide and pyroglutamate,
674 respectively. Predicted consensus secondary structure of *PpCrAMP* using NPS@ server is shown
675 below the amino acid sequence. Lowercase c (orange) and e (blue) indicate random coil and extended
676 strand, respectively.

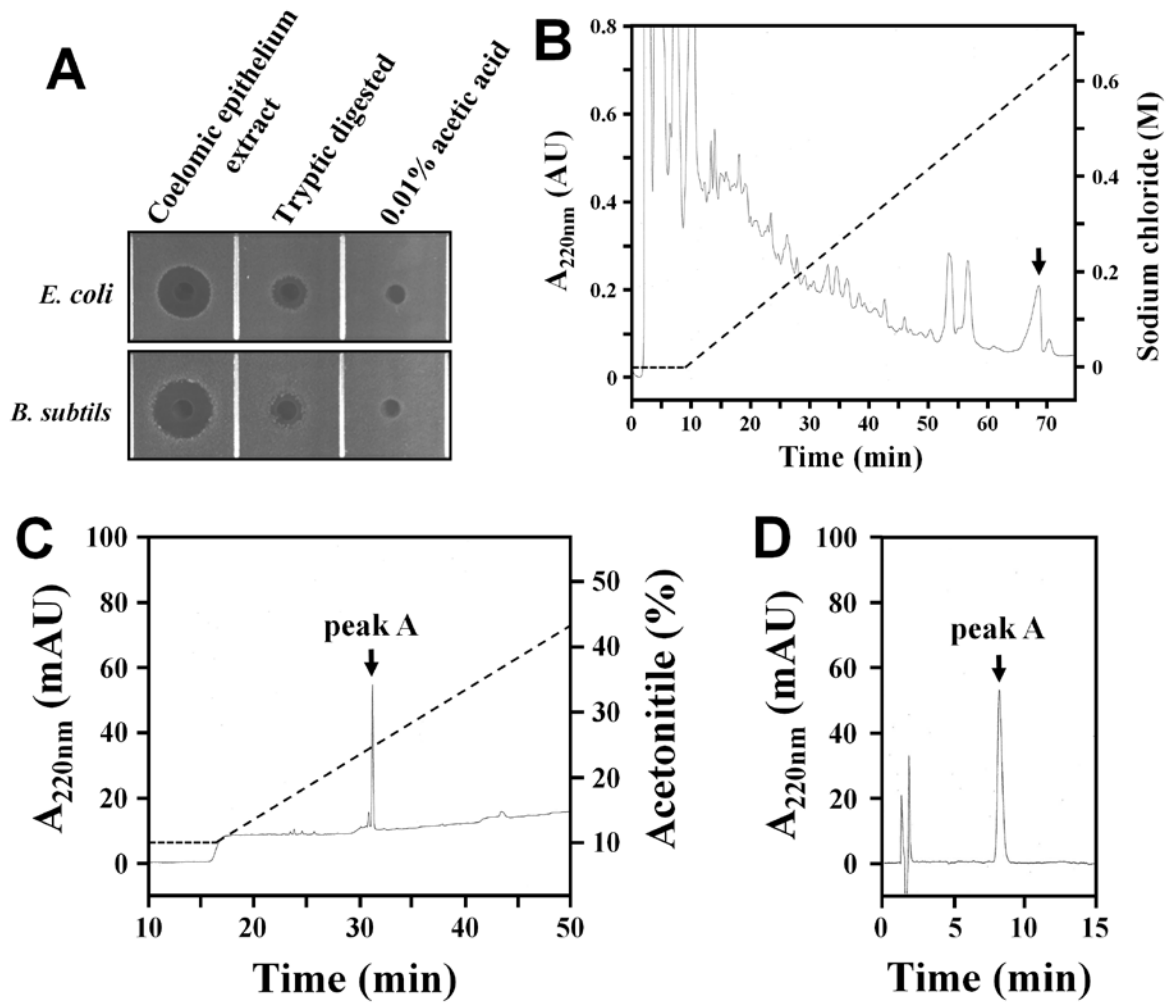
677

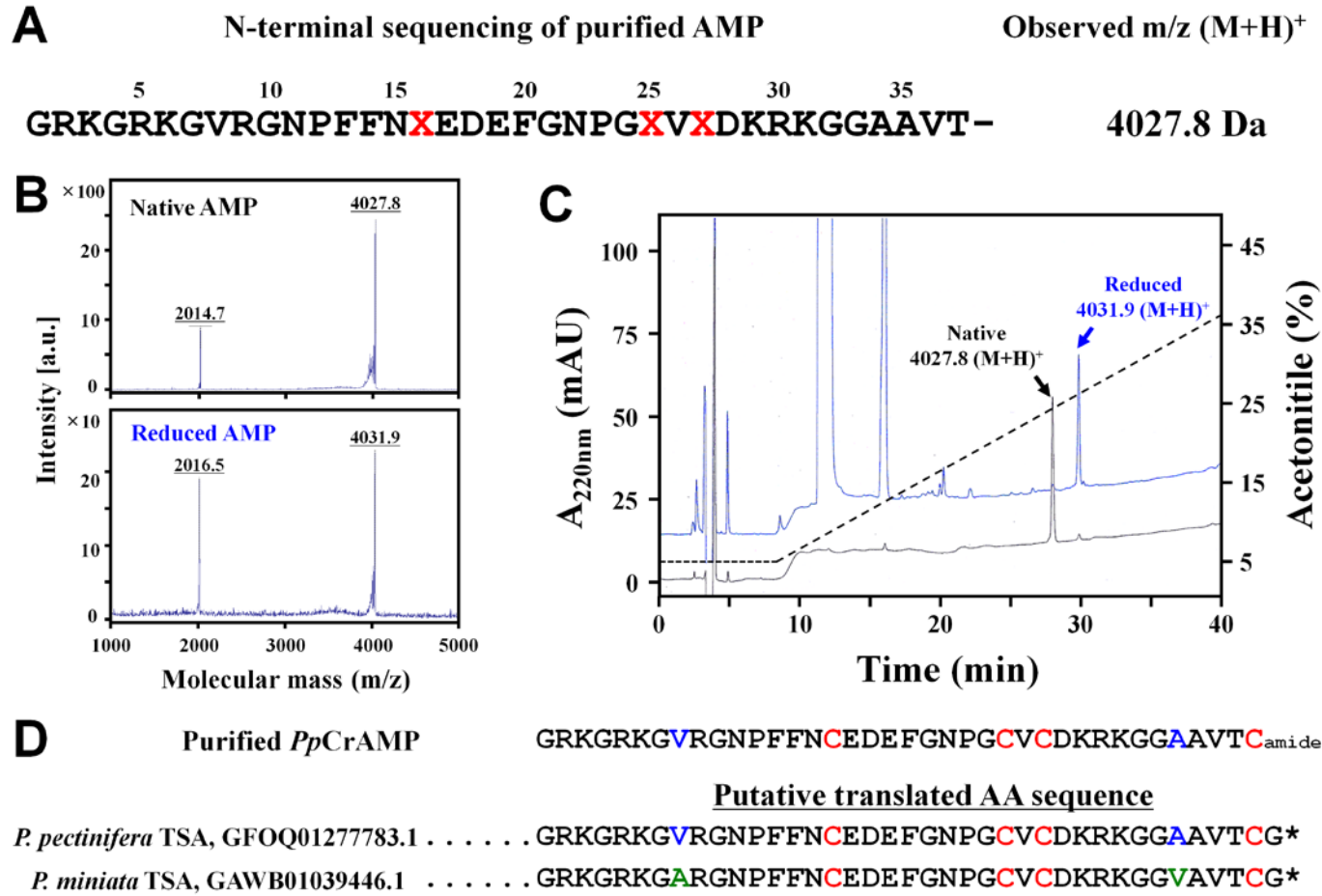
678 **Table legend**

679 **Table 1.** Antimicrobial activity against various microbial strains of synthetic *PpCrAMPs*, including
680 the reduced peptide and peptides with three different combinations of two disulfide bonds

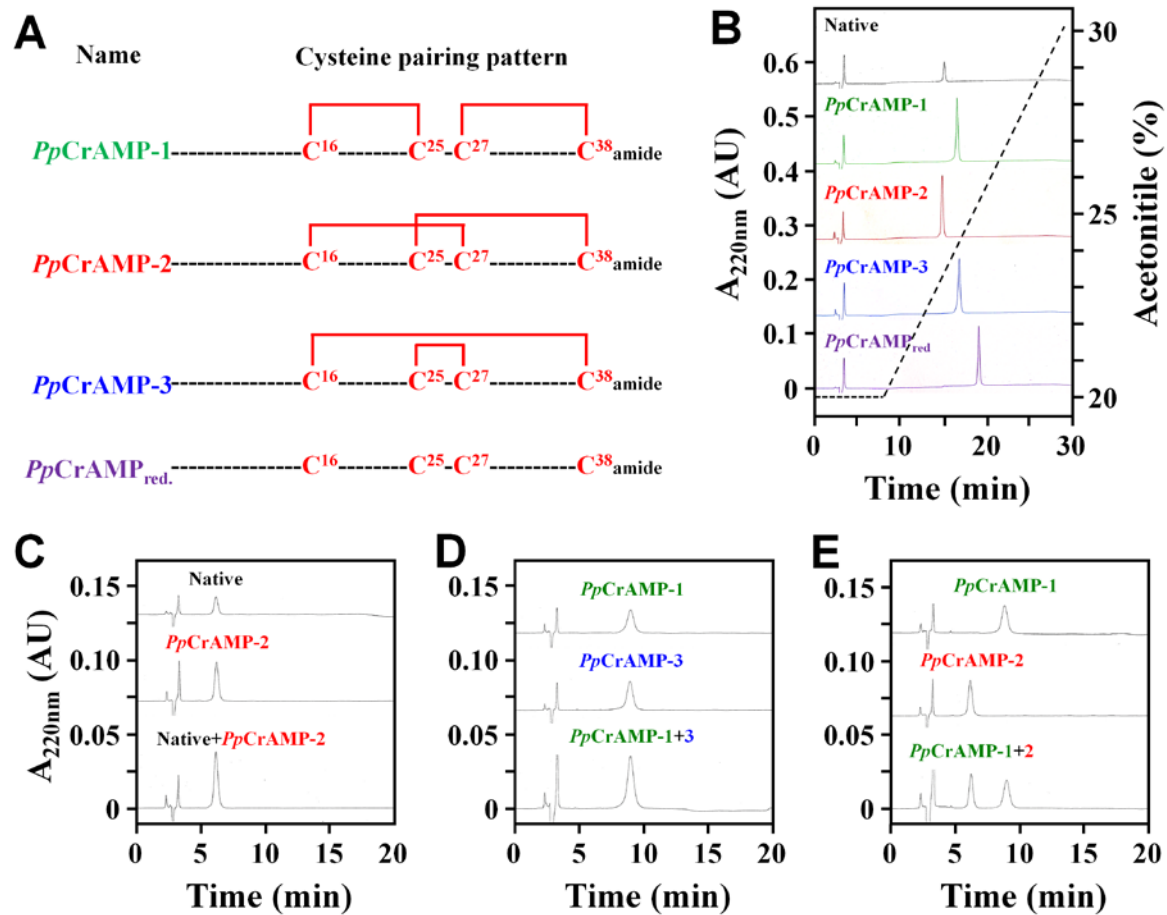
681 **Supplementary table legend**

682 **Supplementary Table S1.** Designations and nucleotide sequences of the primers used in this study

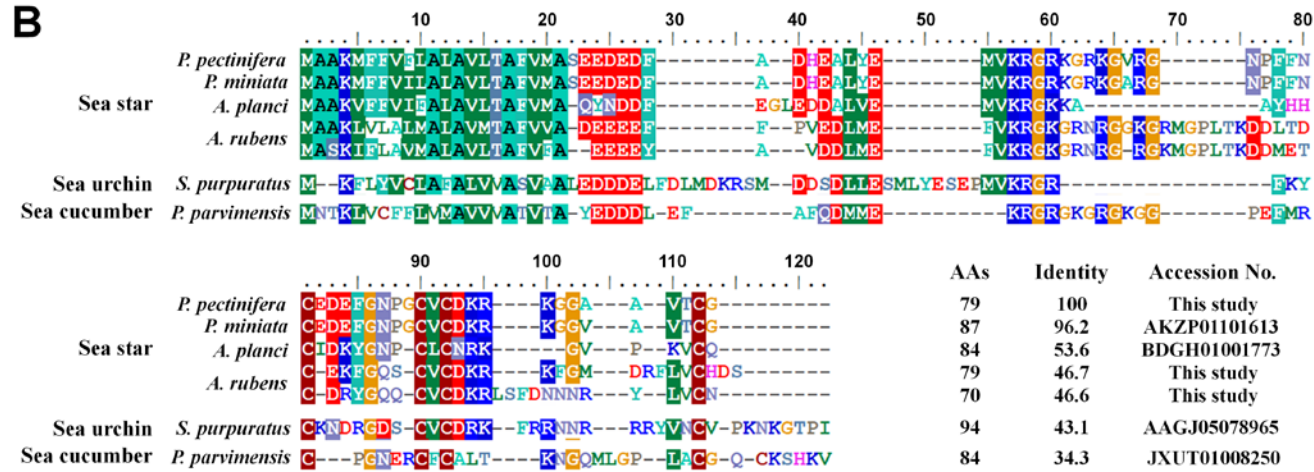
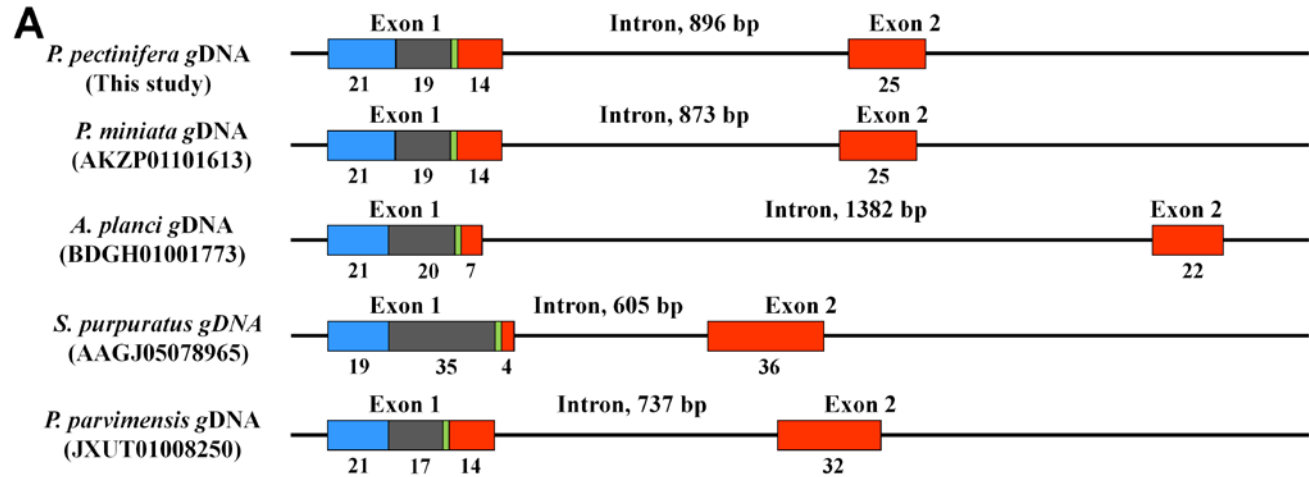


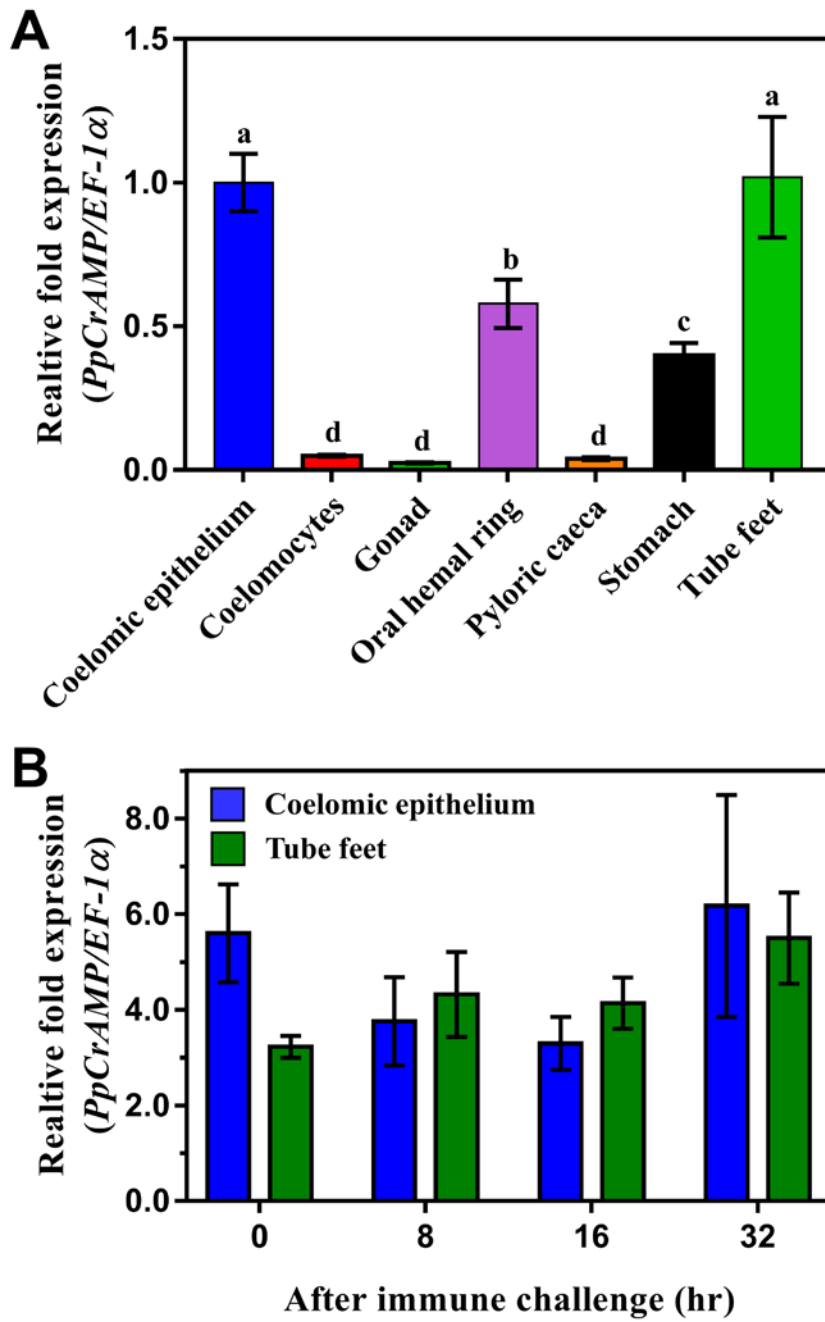


687 Figure 3.



688





696 Figure 7.

Species	Peptide	Sequence	AAs	Cysteine connectivity
<i>P. pectinifera</i>	<i>PpCrAMP</i>	GRKGRKGVRGNPFFN C EDEFGNPG C VCDKRKGGAAV T C a	38	C1-C3 and C2-C4
	<i>Consensus secondary structure prediction</i>	cc		
<i>S. scrofa</i>	<i>Protegrin-1</i>	RGGR L C Y C RRR F C V C VGRa	18	
<i>A. australis</i>	<i>Androctonin</i>	RSV C RQIKI C RRRGG C YY K C TNR P Y	25	
<i>A. gomesiana</i>	<i>Gomesin</i>	pQ C RR L C Y K Q R C V T Y C RGRa	18	C1-C4 and C2-C3
<i>L. polyphemus</i>	<i>Polyphemusin-I</i>	RR W C FR V C YR G F C YR K C Ra	18	
<i>T. tridentatus</i>	<i>Tachyplesin-I</i>	K W C FR V C YR G I C YR R C Ra	17	

697

698 **Table 1.** Antimicrobial activity against various microbial strains using synthetic *PpCrAMPs*, including
 699 a reduced linear peptide and peptides with two disulfide bonds in three different configurations

Microbe	^a Minimal effective concentration (µg/ml)			
	<i>PpCrAMP-1</i>	<i>PpCrAMP-2</i>	<i>PpCrAMP-3</i>	<i>PpCrAMP_{red.}</i>
Gram-positive				
<i>Bacillus subtilis</i> KCTC1021	33.8	22.9	38.3	42.3
<i>Staphylococcus aureus</i> KCTC1621	32.1	15.6	41.2	91.2
<i>Micrococcus luteus</i> KCTC1071	>250	153	>250	82.9
Gram-negative				
<i>Escherichia coli</i> D31	^b ND	ND	ND	ND
<i>Salmonella enterica</i> ATCC13311	8.0	4.5	8.1	8.4
<i>Shigella flexneri</i> KCTC2517	29.8	12.2	31.4	24.2
Marine bacterium (gram-positive)				
<i>Streptococcus iniae</i> FP5229	ND	ND	ND	ND
Marine bacteria (gram-negative)				
<i>Aeromonas hydrophila</i> KCTC2358	ND	107.2	ND	ND
<i>Edwardsiella tarda</i> NUF251	ND	ND	ND	ND
<i>Vibrio parahaemolyticus</i> KCCM41664	ND	>250	ND	ND
Fungus				
<i>Candida albicans</i> KCTC9765	ND	ND	ND	ND

700 ^aAntimicrobial assay were performed in triplicates and the results were averaged.

701 ^bND means not detected in the range of the concentrations tested up to 250 µg/ml of peptides

702 **Supplementary Table S1.** Designations and nucleotide sequences of the primers used in this study

Primers	Nucleotide sequence (5'→3')	Usage
GSP-F1	GGTGTTCAGGGGCAATCCTTT	cDNA cloning
GSP-F2	CAACTGTGAAGACGAGTTCGG	
GSP-R	GCATGTACTTAGCCGCAGG	
Gene F	AACTCGCCTCTCCGAAAA	Gene cloning
Gene R	ACTAGGCCAGATGTGAGCAG	
<i>PpCrAMP</i> qPCR-F	GGTGTTCAGGGGCAATCCTTT	RT-qPCR
<i>PpCrAMP</i> qPCR-R	GGCTCCACCCTTCCTTTTGT	
<i>EF1α</i> qPCR-F	TCAACGACTACCAGCCCCTA	
<i>EF1α</i> qPCR-R	TTCTTGCTAGCCTTCTGGGC	

703

Highlights

- A novel cysteine-rich AMP (*PpCrAMP*) is identified from the starfish *Patiria pectinifera*.
- *PpCrAMP* adopts two disulfide bonds with Cys¹⁶-C²⁷ and Cys²⁵-Cys³⁸ pairings.
- *PpCrAMP* transcripts are highly expressed in the tube feet and the coelomic epithelium.
- *PpCrAMP* gene contains an intron.
- *PpCrAMP* exhibits antimicrobial activity to different bacteria.